Kinetics of Peroxynitric Acid Reactions with Halides at Low pH

Jean-Michel Régimbal and Michael Mozurkewich*

Chemistry Department and Centre for Atmospheric Chemistry, York University, 4700 Keele Street, Toronto, ON, M3J 1P3 Canada

Received: August 25, 1999; In Final Form: May 2, 2000

The oxidation of iodide, bromide, and chloride by peroxynitric acid ($HOONO_2$) was studied by spectroiodometry. The second-order rate constants were found to be 890 (I^-, 295 K), 0.54 (Br^-, 295 K), and 0.0014 M^{-1} s^{-1} (Cl^-, 298.2 K). No pH dependence was observed in any of the systems (pH 1.2−4.9). The temperature and ionic-strength dependencies of the chloride oxidation rate constant are 4.8×10^7 M^{-1} s^{-1} exp(−60 kJ $mol^{-1}/(RT)$) and 6.0×10^{-4} M^{-1} s^{-1} + 1.7×10^{-4} M^{-2} s^{-1} μ, respectively, where μ is the ionic strength. $HOONO_2$ also reduces halogens (X_2), the active species being HO_2, a radical in constant equilibrium with $HOONO_2$. Under most conditions, the reduction can be explained quantitatively with a free-radical mechanism using known rate constants. Reduction by H_2O_2 was not significant. These systems also seem to be affected by reactions in addition to the direct oxidation and free-radical reduction. First, some iodine atoms are stored in a reservoir when initial concentrations of iodide and peroxynitric acid are near stoichiometric values, but we could not identify this reservoir. Second, reaction of $HOONO_2$ with large excesses of KBr (in the 10^{-2} M range) gave inordinately fast and variable bromide oxidation. The addition of Cu^{2+} suppressed this at pH 1.7, suggesting an additional oxidation mechanism that involves HO_2. On the basis of the above results, the potential role of $HOONO_2$ in sea-salt chemistry has been evaluated. Given typical marine boundary layer conditions, it should be negligible in warm, clean, remote oceanic areas. In polluted coastal regions and/or at low temperatures, it might become marginally significant compared to other known reactions leading to halogen release from sea-salt particles.

Introduction

There is a growing interest in the chemistry of chlorine and bromine atoms in both the marine boundary layer and the Arctic troposphere. Chlorine has drawn attention mostly because of the fact that sea-salt particles have long been known to have a $[Cl^-]$:$[Na^+]$ ratio significantly lower than that of seawater.[1] If the missing chloride were to enter the gas phase as photolabile compounds, it could give rise to enough gas-phase chlorine atoms to compete efficiently with OH as the starting point of oxidation processes in the marine boundary layer. Sparse field measurements have provided ground for believing that there might indeed be substantial levels of Cl_2 and/or HOCl in the marine boundary layer at night, enough to release vast numbers of Cl atoms at sunrise.[2,3] Bromine is also of great interest for the study of the disappearance of ground-level ozone observed at polar sunrise in the Arctic, as it has been linked to severe ozone depletion events.[4]

So far, there have been two theories to explain the chloride deficit observed in sea-salt particles.[5] The first one is acid displacement, according to which the condensation of sulfuric and nitric acids on the particles lowers their pH and drives chloride out as HCl(g). If this mechanism were dominant, little chlorine would be produced, for gas-phase HCl is a species of limited atmospheric reactivity that is removed mostly by wet deposition. The second theory involves the oxidation of the chloride within the particle, making a volatile, photolabile species such as HOCl, Cl_2 or BrCl. In the past, the oxidants that have been studied have been for the most part members of the NO_y family, especially N_2O_5 and NO_3, though O_3 has recently come under scrutiny as well.[6,7] Another interesting theory has also been put forward that would involve not only O_3 but also bromide and HO_2 as key chloride removers, with BrCl as the volatile compound being predominantly released.[8] Despite numerous encouraging results, our understanding of this process remains incomplete.

One NO_y species that has not yet been extensively studied is peroxynitric acid, $HOONO_2$. It is always present in the atmosphere, even if at low levels, because it is in equilibrium with its ubiquitous parent radicals, HO_2 and NO_2.[9] Our earlier work on its thermal decay in acidic solutions showed it had a Henry's law constant of 12 600 M atm^{-1} at 298 K and a lifetime of tens of minutes, determined by the disproportionation of HO_2 and NO_2 into more stable products in a mechanism described by reactions 1−4.[10] Thermal decay also proved to be highly variable, apparently because of reactions of the radical intermediates with trace transition metals.

$$HOONO_2 \rightleftharpoons HO_2 + NO_2 \quad (1)$$

$$2HO_2 \rightarrow H_2O_2 + O_2 \quad (2)$$

$$2NO_2 + H_2O \rightarrow HNO_2 + H^+ + NO_3^- \quad (3)$$

$$HNO_2 + H_2O_2 \rightarrow H^+ + NO_3^- + H_2O \quad (4)$$

Less acidic solutions lead to dramatically shorter lifetimes, as the conjugate base peroxynitrate (NO_4^-) decays to O_2 and NO_2^- in a matter of seconds. $HOONO_2$ has a pK_a of 5.85.[11] We have shown previously that it is a potent aqueous-phase oxidant whose reduction potential places it above chlorine in the reactivity series. Furthermore, it has been reported that it

* Corresponding author. E-mail: mozurkew@yorku.ca.

10.1021/jp9930301 CCC: $19.00
Published on Web 06/27/2000

does oxidize chloride.[12] The oxidation of iodide by peroxynitric acid is already documented; the acid itself oxidizes iodide with a rate constant of 840 ± 50 M^{-1} s^{-1}, while NO_4^- does so at only 56 M^{-1} s^{-1} at pH 7.1.[13]

We have studied the decay of $HOONO_2$ in the presence of chloride, bromide, and iodide as well as the production of iodine and bromine in various systems. Of particular interest was the fact that $HOONO_2$ acted not only as an oxidant but also as a reductant. In fact, it proved kinetically more efficient as a reducing agent than the hydrogen peroxide present in the systems we studied.

Reactions and equilibria (5)−(9) are expected to take place with all three halides. In the following, for example, reaction 5(I) and k_5(I) will stand for reaction 5 with X = I and the corresponding rate constant, respectively.

$$HOONO_2 + X^- \rightarrow NO_3^- + HOX \quad (5)$$

$$X_2 + H_2O \rightleftharpoons HOX + X^- + H^+ \quad (6)$$

$$X_2 + X^- \rightleftharpoons X_3^- \quad (7)$$

$$H_2O_2 + X^- + H^+ \rightarrow H_2O + HOX \quad (8)$$

$$H_2O_2 + HOX \rightarrow H_2O + O_2 + X^- + H^+ \quad (9)$$

Experimental Section

Material and Solutions. All experiments used water that was first deionized and then redistilled from $KMnO_4$ in an all-glass apparatus. KI, NaOH, ammonium molybdate, $CuSO_4 \cdot 5H_2O$, 70% HNO_3, 85% H_3PO_4, 98% H_2SO_4, pH 4.00 phthalate buffer (all from BDH), $NaNO_3$ (BDH and Caledon), 30% H_2O_2 (BDH and Fisher Scientific), glacial CH_3COOH (Caledon), Na_2EDTA, $ClCH_2COOH$ (both from Fisher Scientific), pH 2.00 HCl/KCl standard solution (VWR), and $NaNO_2$ (J. T. Baker) were used as supplied. Other buffers were prepared from the appropriate acids and NaOH and were typically 0.10 M. Varying the nature and/or concentration of the buffer with the bromide and chloride systems did not show a measurable effect on the chemistry.

$HOONO_2$ Synthesis. $HOONO_2$ was prepared with a slightly scaled-up version of the synthesis described by Appelman and Gosztola,[12] but with $HClO_4$ replaced by 70% HNO_3. The resulting solution will be referred to as the reaction mixture. It was stored at −18 °C and significant amounts of $HOONO_2$ remained for several weeks. Iodometric titrations gave average $HOONO_2$ and H_2O_2 concentrations of 1.6 and 2.4−3.0 M in the reaction mixture, respectively.

For kinetic studies, the reaction mixture was diluted by factors of the order of 10^3. For the classical and kinetic spectroiodometry procedures, 70.0 μL of the reaction mixture were added to 50.00 mL of the appropriate HNO_3 or buffer solution. In the flow experiments, 20.0−100 μL of reaction mixture were added to 50 mL of the appropriate HNO_3 or buffer solution. Na_2EDTA (1.0 mM) was added to these dilute reaction mixtures to stabilize $HOONO_2$.[10]

Apparatus. For all experiments, a Hewlett-Packard 8452A diode-array UV−visible spectrophotometer was used, with a 1 cm path length quartz cell. It can take simultaneous readings at 2 nm intervals in the 190−820 nm range but, normally, only the 280−360 nm range was used. It was equipped with a HP Peltier temperature-controller, model 89090A, that maintained the cell temperature at 25.0 °C and stirred the solution at 300−600 rpm with a small magnet cast in glass or Teflon. When temperature control was needed in the classical and flow experiments, a Neslab RTE−210 thermostated bath was used to circulate fluid through a 50-mL jacketed beaker equipped with a magnetic stirrer. The temperature was systematically controlled in chloride experiments, with a default value of 25.0 °C. Others were carried out at room temperature, 22 ± 1 °C. pH measurements were made with a pH meter (model 10 Accumet, Fisher Scientific).

Spectroiodometry—Basic Principles. Kinetic studies have been done by measuring spectrophotometrically the triiodide produced by reactions 5(I)−7(I). This has been described in detail elsewhere.[10] Briefly, part of the dilute reaction mixture is mixed with a large volume of KI solution. Reaction 5(I) takes place, the large I^- excess converting $HOONO_2$ into iodine and triiodide. The I_3^- absorption is monitored at 352 nm (ϵ = 26 400 M^{-1} cm^{-1}).[14] Reaction 8(I) is almost negligible, unless a catalyst is added to the KI solution.

Three different forms of spectroiodometry were used. Classical spectroiodometry was used for $HOONO_2$ lifetimes of 20 min or more and flow spectroiodometry for shorter ones (down to 20 s). In both cases, the I_3^- absorbance can be directly related to the $HOONO_2$ concentration in the dilute reaction mixture. The third technique, kinetic spectroiodometry, helped measure the rate constant of reaction 5(I). The three variations of spectroiodometry developed so far have been described elsewhere;[10] the following is just a short summary of each.

Classical Spectroiodometry. In classical spectroiodometry, an aliquot of the dilute reaction mixture is transferred to an 8 mM KI solution being monitored spectrophotometrically; the quick absorbance rise is then related to the $HOONO_2$ concentration in the dilute reaction mixture. The subsequent addition of ammonium molybdate catalyst to the cell allowed us to measure the H_2O_2 concentration. Repeating the procedure several times with the same dilute reaction mixture led to the determination of peroxynitric acid's observed first-order decay rate constant and to the concurrent H_2O_2 decay.

Flow Spectroiodometry. Flow spectroiodometry is a variation of the previous technique where the dilute reaction mixture and an 8.73 mM KI solution are continuously drawn and mixed together in a flow system. By the time the combined flows reach the spectrophotometer cell, reaction 5(I) is over and $HOONO_2$ can be quantified through I_3^- absorbance.

Kinetic Spectroiodometry. A small aliquot of partially diluted $HOONO_2$ solution (intermediate reaction mixture) is added to acidified or buffered KI solution in the cell and the growth of both I_2 and I_3^- is monitored spectrophotometrically. Figure 1 shows a typical time trace. The first 10 s of data serve as an internal blank, and the corrected absorbances are then converted into concentrations of I_2 and I_3^-. Afterward, curve fitting is used to find the appropriate rate constant. The height of the final plateau is related to the yield.

All the uncertainties based on our measurements are given in the text as the 95% confidence level determined from sample standard deviation. We assume that all the uncertainties found in the literature were also for this confidence level.

In the following, the notation X(0) stands for the sum of all oxidized forms of a halogen: X_3^-, X_2, HOX, and OX^-. Given our experimental conditions, only the first two mattered in the mass balance of iodide and bromide systems; HOCl was significant in the chloride systems. Rate constants related to this work and used in modeling are all listed in Table 1.

Results and Discussion

Iodide System. This system was studied over a wide range of KI concentrations that were broken into three broad categories

TABLE 1: Rate Constants Used in This Work[a]

reaction	rate constants	ref
(1) $HOONO_2 \rightarrow HO_2 + NO_2$	0.017 ± 0.003 (22 °C) 0.026 ± 0.002 (25 °C)	10
(−1) $HO_2 + NO_2 \rightarrow HOONO_2$	1.8×10^9	11
(2) $2HO_2 \rightarrow H_2O_2 + O_2$	$(9.0 \pm 0.7) \times 10^5\ M^{-1}\ s^{-1}$	10
(3) $2NO_2 + H_2O \rightarrow HNO_2 + H^+ + NO_3^-$	$(6.5 \pm 3.5) \times 10^7\ M^{-1}\ s^{-1}$	10
(4) $HNO_2 + H_2O_2 \rightarrow H^+ + NO_3^- + H_2O$	$8.4 \times 10^3\ M^{-2}\ s^{-1}\ [H^+]$	35
(17) $HO_2 + Cu^{2+} \rightarrow H^+ + O_2 + Cu^+$	1.2×10^9	36
(18) $HO_2^+ Cu^+ \rightarrow HO_2^- + Cu^{2+}$	1×10^9	36

	rate constants			
reaction	I	Br	Cl	ref
(5) $HOONO_2 + X^- \rightarrow NO_3^- + HOX$	890 ± 90[b]	0.54 ± 0.08	$(1.4 \pm 0.5) \times 10^{-3}$	this work
(6) $X_2 + H_2O \rightarrow HOX + X^- + H^+$	3	110	11	36, 37
(−6) $HOX + X^- + H^+ \rightarrow X_2 + H_2O$	$4.4 \times 10^{12}\ M^{-2}\ s^{-1}$	$1.6 \times 10^{10}\ M^{-2}\ s^{-1}$	$1.8 \times 10^4\ M^{-2}\ s^{-1}$	36, 37
(7) $X_2 + X^- \rightarrow X_3^-$	$(5.6 \pm 0.6) \times 10^9$	$(8 \pm 2) \times 10^8$	$0.18 \pm 0.02\ M^{-1}$ [b]	17, 38[d]
(−7) $X_3^- \rightarrow X_2 + X^-$	$(7.5 \pm 0.8) \times 10^6$	$(5 \pm 1) \times 10^7$	$5.5 \pm 0.5\ M$[c]	38[d]
(8) $H_2O_2 + X^- + H^+ \rightarrow H_2O + HOX$	$0.012 \pm 0.002\ M^{-1}\ s^{-1}$ $+ 0.168 \pm 0.002\ M^{-2}\ s^{-1}\ [H^+]$	$(2.7 \pm 0.6) \times 10^{-7}\ M^{-1}\ s^{-1}$ $+ (2.36 \pm 0.04) \times 10^{-4}\ M^{-2}\ s^{-1}\ [H^+]$	$(8.2 \pm 0.7) \times 10^{-7}\ M^{-2}\ s^{-1}\ [H^+]$	39, 40[e]
(9) $H_2O_2 + HOX \rightarrow H_2O + O_2 + X^- + H^+$	$37 \pm 4\ M^{-1}\ s^{-1}$ $+ (1.58 \pm 0.14) \times 10^{-3}\ s^{-1}\ [H^+]^{-1}$	$5.8 \times 10^4\ M^{-1}\ s^{-1}$	NA	41, 42[f]
(11) $HO_2 + X_2 \rightarrow H^+ + O_2 + X_2^-$	1.8×10^7	1.1×10^8	1.0×10^9	18
(12) $X_2^- \rightarrow X^- + X$	1×10^5	4×10^4	NA	18
(−12) $X^- + X \rightarrow X_2^-$	1.1×10^{10}	9×10^9	NA	18
(13) $2X \rightarrow X_2$	$8 \times 10^9\ M^{-1}\ s^{-1}$	NA	$1.0 \times 10^8\ M^{-1}\ s^{-1}$	18
(14) $2X_2^- \rightarrow X_3^- + X^-$	$3 \times 10^9\ M^{-1}\ s^{-1}$	$2 \times 10^9\ M^{-1}\ s^{-1}$	$1 \times 10^9\ M^{-1}\ s^{-1}$	18
(15) $NO_2^- + X \rightarrow NO_2 + X^-$	8.8×10^9	NA	NA	18
(−15) $NO_2 + X^- \rightarrow NO_2^- + X$	1.1×10^5	NA	NA	18
(16) $NO_2^- + X_2^- \rightarrow NO_2 + 2X^-$	NA	2×10^7	2.5×10^8	18
(19) $H_2O_2 + X_2 \rightarrow O_2 + 2X^- + 2H^+$	NA	NA	180	20
(20) $HOCl + Br^- \rightarrow BrCl + OH^-$	2.5×10^3			25
(21) $Cl_2 + Br^- \rightarrow BrCl_2^-$	$(6.5 \pm 1.1) \times 10^9$			17
(22) $BrCl + Cl^- \rightarrow BrCl_2^-$	$K = 6.0 \pm 0.3\ M^{-1}$ [b]			17

[a] Units are in $M^{-2}\ s^{-1}$, $M^{-1}\ s^{-1}$, or s^{-1}, as appropriate and have been included only where they might otherwise be ambiguous. [b] Reference 13 gives $840 \pm 50\ s^{-1}$. [c] Equilibrium constant. [d] Reference 38 for I^- and Br^-, 17 for Cl^-. Ruasse et al. reported $k_7(Br) = 1.5 \times 10^9\ M^{-1}\ s^{-1}$ in their Table 4, but this gives $K_7(Br) = 30\ M^{-1}$, off by a factor of 2. They were unable to measure $k_7(Br)$ directly, but instead calculated it from their $k^-_7(Br)$ measurement and the known $K_7(Br)$; we deemed the latter to be more reliable and recalculated $k_7(Br)$ using $K_7(Br) = 16.1 \pm 0.3\ M^{-1}$.[17] [e] $k_8(I)$ obtained by reanalyzing the data in Table 1 of ref 39 by linear regression; $k_8(Br)$ found by reanalyzing the data in Table 2 of ref 40 with linear regression and $k_8(Cl)$ from Table 3 of ref 40. [f] For $k_9(I)$, the data in Tables 1 and 2 of ref 41 were reanalyzed and then adjusted to account for a reaction involving HOI instead of OI^-. $k_9(Br)$ from ref 42.

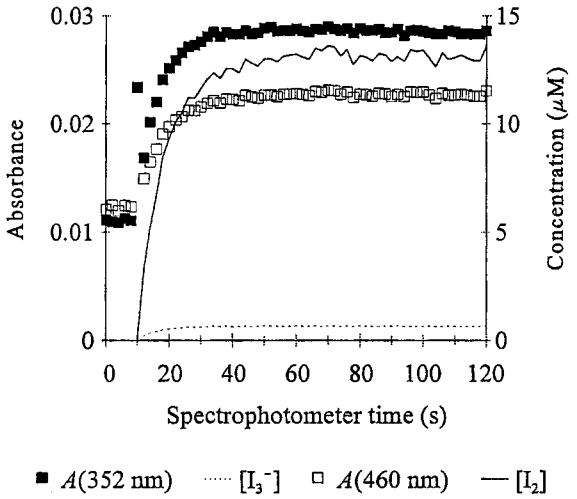

Figure 1. Example of a time trace in kinetic spectroiodometry. Intermediate reaction mixture aliquot added at $t = 10$ s. I_3^- measured at 352 nm, I_2 at 460 nm. Conditions: 23 μM $HOONO_2$, 96 μM KI, pH 1.6.

based on the relative concentrations of $HOONO_2$ and KI; the experimental conditions for each are listed in Table 2.

Comparing runs done by classical and kinetic spectroiodometry showed that when KI was in large excess over $HOONO_2$, the reaction quantitatively produced I(0). With 13−27 μM $HOONO_2$ in the dilute reaction mixture, this proved true down to approximately 500 μM KI. Below that threshold, yields dropped markedly, as shown in Figure 2. Despite the scatter in the data, it is clear that the effect is real. At 100 μM KI, the yield is 80% at pH 1.6 and 60% at pH 3.1. Since KI is still well in excess over $HOONO_2$ in this region, by a factor of 20:1 to 60:1, something must prevent $HOONO_2$ from being fully converted to I(0). Given the short time scale of the experiments, thermal decay could not have accounted for the lower yield. The most likely reason is that I(0) was being reduced by $HOONO_2$. Note that at higher KI concentrations, the yield plateaus slightly below 100%. The reason might be a small systematic difference between kinetic and classical spectroiodometries, the 100% yield level being set on the basis of numbers supplied by the second technique.

It was also found by flow spectroiodometry that when catalytic amounts of KI were present in the dilute reaction mixture, the decay of peroxynitric acid was accelerated. However, the observed decay rate constant reached a maximum of 0.020 s^{-1} with about 100−200 μM KI and then slowly decreased, as illustrated in Figure 3. Furthermore, with 100 μM KI and above, I_3^- became visible in the dilute reaction mixture as soon as $HOONO_2$ and KI were mixed and survived even when the spectrophotometer time trace showed that no decay was taking place anymore, i.e., that $HOONO_2$ had totally disappeared from the solution. This particular range of KI concentrations (∼100−500 μM) was termed "near-stoichiometric," to distinguish it from properly catalytic ones, with which no significant levels of I(0) could be measured after peroxynitric acid's disappearance. The fact that the observed decay rate constant more or less reached a plateau with a value about the same as for the rate constant of reaction 1 ($0.017 \pm 0.003\ s^{-1}$

TABLE 2: Experimental Conditions for the Iodide and Bromide Systems[a]

	experiments	method	$[HOONO_2]_o$ (mM)	$[X^-]_o$ (mM)	$[X^-]_o$:$[HOONO_2]_o$
I^-	Large excess	K	0.027	3−27	100−1000
	moderate excess	K	0.011−0.038	0.05−3	2.5−200
	near-stoichiometricto catalytic	F	0.19−2.7[b]	0.006−0.5	0.01−2.1
Br^-	catalytic	C	0.3−6	0.01−3	0.01−2.3
	catalytic	F	0.3−4	1−20	0.6−70
	semicatalytic	F	0.6	10−50	20−90
	spectrobromometric	B	0.0012−0.044	5−400	275−74000

[a] Methods are identified as follows: B, spectrobromometry; C, classical spectroiodometry; F, flow spectroiodometry; K, kinetic spectroiodometry (with support from classical spectroiodometry). [b] Most experiments done with either ~0.30 or ~0.51 mM $HOONO_2$.

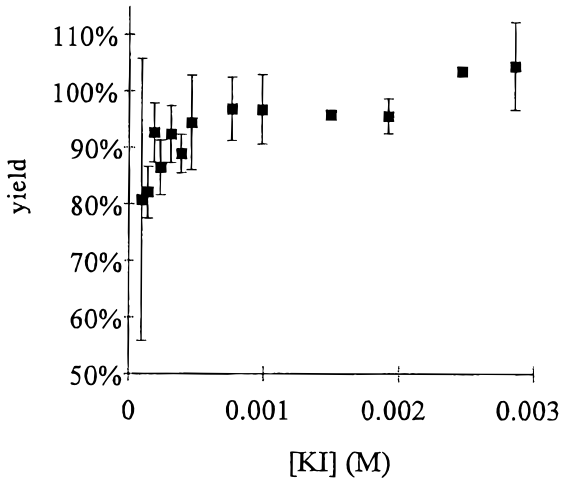

Figure 2. Conversion of 14 ± 1 μM $HOONO_2$ to I(0) in kinetic spectroiodometry at pH 1.6. Error bars represent one sample standard deviation for triplicate measurements. 100% conversion based on classical spectroiodometry.

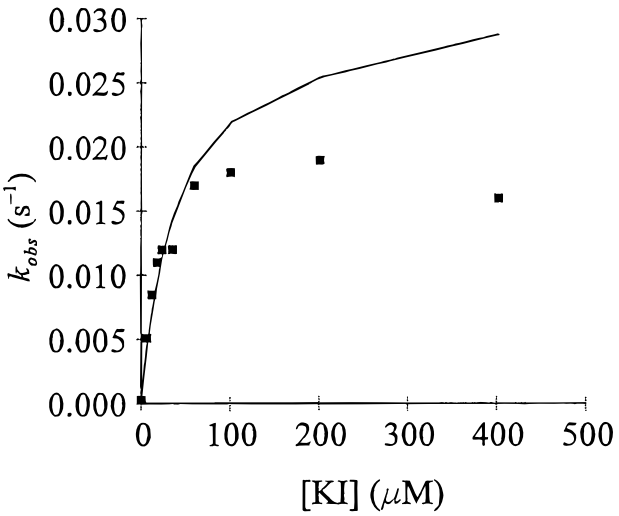

Figure 3. Influence of catalytic to near-stoichiometric amounts of KI in the dilute reaction mixture on the signal's observed decay rate constant for an initial 320 ± 20 μM $HOONO_2$ at pH 1.68 ± 0.01. Runs at higher KI concentrations (□) were fit with eq I to account for steady-state levels of I(0). The line represents k_{obs} as predicted by the radical-reduction model with a standard 300 μM $HOONO_2$.

at room temperature) suggested that the reduction proceeded through HO_2 and/or NO_2 formed by reaction 1. The reducing agent could not have been H_2O_2 since, given the experimental conditions, I(0) has a lifetime of the order of several hours against H_2O_2, reaction 9(I).

The observed $HOONO_2$ decay rate constants presented in Figure 3 were found by fitting the data to eq I, keeping in mind that the signal corresponded to the sum of $HOONO_2$ and I(0). A_o is the I_3^- absorbance after the KI was added to the dilute reaction mixture and A_∞ is the absorbance of the I(0) that remains after all $HOONO_2$ has disappeared. Equation I is based on the assumption that A_∞ corresponded to a steady-state amount of I(0) that was formed very quickly.

$$A = (A_o - A_\infty)e^{-k_{obs}t} + A_\infty \quad \text{(I)}$$

We attempted to fit kinetic spectroiodometry time traces for moderate excesses of KI using a direct reduction, reaction 10, in addition to reactions 1−7(I). This gave reproducible values

$$HOONO_2 + I_2 + H_2O \; 6\; NO_3^- + O_2 + 2I^- + 2H^+ \quad (10)$$

of k_5(I), with an average of 890 ± 90 M^{-1} s^{-1}, in agreement with the value of 840 ± 50 M^{-1} s^{-1} reported by Goldstein and Czapski.[15] k_5(I) did not vary significantly between pH 1.6 and 3.1. However, the values obtained for k_{10} varied over several orders of magnitude. The oxidation rate constant k_5(I) was primarily determined by the initial I(0) production, while the reduction rate constant k_{10} depended mostly on the final I(0) yield.

As an alternative, we constructed a radical-reduction model in which we replaced reaction 10 with reactions 11(I)−15(I), using known rate constants from the literature and $k_5(I) = 890$ M^{-1} s^{-1}. The I_2 reduction is initiated by HO_2 in rate-limiting

$$HO_2 + X_2 \rightarrow H^+ + O_2 + X_2^- \quad (11)$$

$$X_2^- \rightleftharpoons X^- + X \quad (12)$$

$$2X \rightarrow X_2 \quad (13)$$

$$2X_2^- \rightarrow X^- + X_3^- \quad (14)$$

$$NO_2^- + X \rightleftharpoons NO_2 + X^- \quad (15)$$

reaction 11(I), then NO_2^- completes the reduction. Below approximately 30 μM KI, this model produces rate constants that are slightly smaller than the ones we have observed. At higher [KI], the model predicts a signal decay rate constant that becomes increasingly larger than the one observed (see Figure 3); the difference is pronounced above 100 μM KI. Qualitatively, both the behavior of the experiments and the model can be explained as follows. The signal decay results from two processes: reactions 1 and 11 with the former being rate-limiting. Thus, the observed rate constant is expected to reach a maximum value equal to $2k_1$ (0.034 s^{-1} at the temperature used in Figure 3). I(0) regeneration by reactions 13 and 14 causes the actual decay to be somewhat smaller than this limit. The model shows a slight dependence of decay rate on initial $[HOONO_2]$; a factor of 6 increase in concentration produces a 10% reduction in k_{obs}. This is because of an increase in the

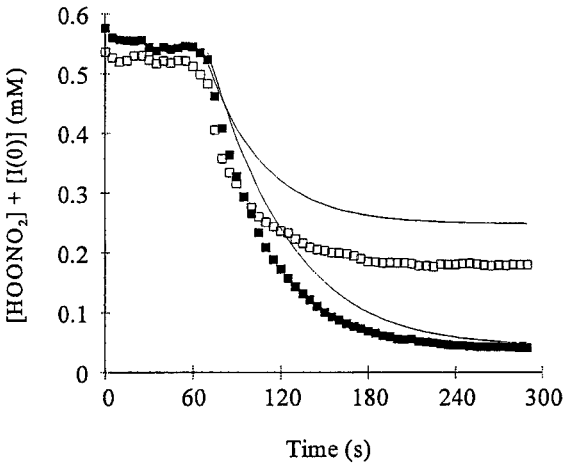

Figure 4. Comparison of data (squares) and radical-reduction model (lines) in the near-stoichiometric [KI] range. $HOONO_2$ is first monitored for a minute in the dilute reaction mixture before adding KI, here either 0.102 mM (■) or 0.510 mM (□). Done at pH 1.78 ± 0.01.

relative importance of reactions 13 and 14 at higher radical concentrations.

We cannot explain the difference between the experimental and modeled decay rates when [KI] ≈ [$HOONO_2$]. Furthermore, the model substantially overestimates the amount of I(0) that survives $HOONO_2$, as illustrated in Figure 4. This is particularly striking at 0.51 mM KI, with an observed final I(0) yield of 70 ± 2% and a modeled one of over 96%. It was obvious that the model was incomplete; three possibilities were considered: (1) a loss of oxidative efficiency at the higher I^- concentrations, (2) other I(0) reduction pathways, or (3) a tying-up of iodine atoms in reservoirs. Attempts to modify the radical-reduction model showed that the oxidation−reduction cycle was so efficient that the only way to explain the lower I(0) yields was to favor the third option, that of an iodine reservoir that would not contribute to the signal once the dilute reaction mixture was mixed with flow spectroiodometry's KI eluent. However, we have not been able to identify a suitable reservoir.

In summary, the behavior of $HOONO_2$ in acidic iodide solutions can be adequately explained outside the near-stoichiometric range of 0.1−0.5 mM KI. Above that range, it reacts quantitatively with iodide to make I(0); below, a catalytic cycle involving reactions 1−3, 5(I)−7(I), and 11(I)−15(I) accounts well for observations. In the near-stoichiometric range, the signal's decay is slower than expected and an iodine reservoir invisible to spectroiodometry is probably being formed. We were unable to identify the reservoir.

Bromide System. As for the iodide system, experiments done with bromide covered a wide range of conditions; these are listed in Table 2. Experiments with catalytic amounts of KBr were performed using both classical- and flow-spectroiodometry. The two techniques gave slightly different values for the observed second-order rate constant, as shown in Figure 5. We favor those measurements done with flow spectroiodometry, for they covered a wider KBr concentration range and were also done in a region where peroxynitric acid's highly variable thermal decay would be less likely to interfere with results. Classical spectroiodometry, on the other hand, proved useful in showing that H_2O_2 played at most a secondary role (reaction 9(Br)) in the reduction of Br(0), for 56 stoichiometric ratios S (defined as $d[H_2O_2]/d[HOONO_2]$) averaged to 0.23 ± 0.06. This meant that $HOONO_2$ was also responsible for the reduction and that k_5(Br) was half the observed second-order reaction rate constant,

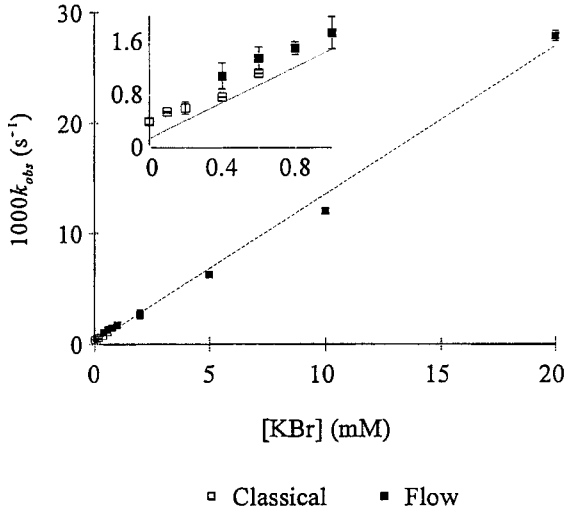

Figure 5. Determination of the oxidation rate constant of bromide by $HOONO_2$, k_5(Br), with two different spectroiodometric techniques. k_{obs} stands for peroxynitric acid's observed first-order decay rate constant. Conditions: 1.8 ± 0.2 mM $HOONO_2$ in 0.10 M phosphate buffer at pH 2.21 (□) and 0.64 ± 0.04 mM $HOONO_2$ in phosphate buffer at pH 2.17 (■). The inset is a detail of the larger graph at low [KBr]. Error bars represent one sample standard deviation.

i.e., 0.54 ± 0.08 M^{-1} s^{-1}. No pH dependence could be discerned between pH 1.70 and 4.92.

A second series of experiments was made with higher KBr concentrations in the semicatalytic range. A dilute reaction mixture containing about 0.6 mM peroxynitric acid at pH 2.00 ± 0.01 was first monitored for 90 s by flow spectroiodometry. A small KBr solution aliquot was then added to it, enough to bring the Br^- concentration to 10−50 mM. The result was the immediate and visible formation of Br_3^-. This Br(0) stayed in the dilute reaction mixture long after all $HOONO_2$ had been consumed, though it would slowly decay on its own. Note that Br(0) in the dilute reaction mixture is quantitatively converted to I(0) once it mingles with the KI eluent.[16] The oxidation rate constant was approximated by fitting the data to eq II.

$$A = (A_o - A_\infty)e^{-k_{obs}t} + A_{res}e^{-k_{res}t} \qquad \text{(II)}$$

$A_o - A_{res}$ is related to $[HOONO_2]_o$, A_{res} to the steady-state Br(0) concentration, and k_{res} to the latter's slow decay. The values of k_{obs} led to an average oxidation rate constant k_5(Br) of 0.60 ± 0.18 M^{-1} s^{-1}, in agreement with those obtained with catalytic amounts of KBr. Between 10 and 60 mM KBr, the yield of residual Br(0) amounted to (4.4 ± 1.4) × 10^{-3} [KBr] for 0.52 ± 0.06 mM $HOONO_2$.

These semicatalytic results were modeled using the radical-reduction model. With the intermediate KBr concentration of 30 mM, the agreement between model and data was good, both giving 0.15 mM of residual Br(0). However, there were some discrepancies as to the yield of residual Br(0) at 10 and 50 mM. At 10 mM KBr, the predicted yield was only 0.010 ± 0.002 mM vs the observed 0.050 ± 0.002 mM; at 50 mM, it was 0.269 ± 0.001 mM vs 0.224 ± 0.003 mM.

Several experiments were carried out at even higher KBr concentrations and pH 1.6−3.1, using spectrobromometry. This technique was essentially kinetic spectroiodometry where the iodide was replaced by a large enough excess of KBr to produce measurable quantities of Br_3^- inside the spectrophotometer cell (cf. Table 2). Br_3^- was monitored by its 266 nm absorption peak (ϵ = 40 900 ± 400 M^{-1} cm^{-1}).[17] These experiments were characterized by serious reproducibility problems. Yet, it was

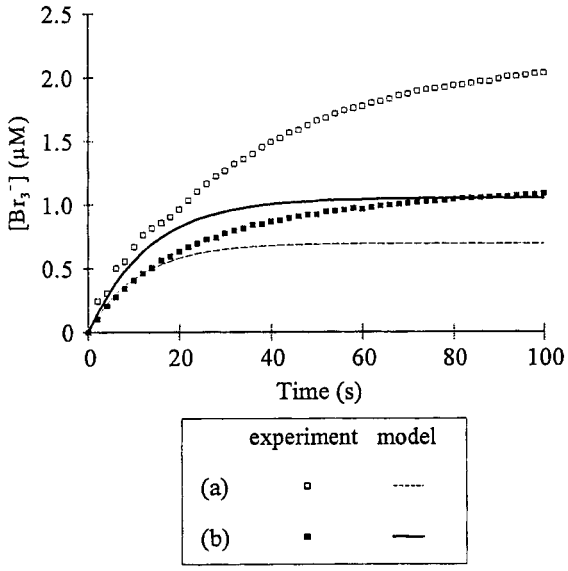

Figure 6. Modeling spectrobomometric data. The lines are model predictions based on our current understanding of the system with (a) 8.8 μM $HOONO_2$ and no $CuSO_4$ and (b) 8.3 μM $HOONO_2$ and 9.7 mM $CuSO_4$. $k_5(Br) = 0.6\ M^{-1}\ s^{-1}$, 25.1 mM KBr, 14 μM H_2O_2 and pH 1.7 ± 0.1 in both cases.

quite clear that the data could not be fitted with $k_5(Br) \approx 0.6\ M^{-1}\ s^{-1}$, contrary to the two previous techniques. In a total of 23 runs, the $k_5(Br)$ values required to fit the data ranged from 0.7 to 5.4 $M^{-1}\ s^{-1}$, with an average of $1.4 \pm 0.5\ M^{-1}\ s^{-1}$, twice as much as expected. It should be noted that the final reduction step in the bromide system is different from the one in the iodide system, as reaction 16 replaces reaction 15(Br).[18]

$$NO_2^- + X_2^- \rightarrow NO_2 + 2X^- \qquad (16)$$

When studying thermal decay[10] and iodine reduction, we had come to interpret experimental lack of reproducibility as a sign of radical chemistry. To determine whether it was the case in spectrobromometry, several runs were done with the addition of 10 mM $CuSO_4$ to the spectrophotometer cell to scavenge HO_2 radicals through reactions 17 and 18; under these conditions, $HOONO_2$ lifetimes against Cu^{2+} and Br^- were comparable. We do not know of any other reaction of either Cu^{2+} or

$$HO_2 + Cu^{2+} \rightarrow H^+ + O_2 + Cu^+ \qquad (17)$$

$$HO_2 + H^+ + Cu^+ \rightarrow H_2O_2 + Cu^{2+} \qquad (18)$$

Cu^+ that could significantly affect the present system. It is already known that Cu^+ and NO_2 do not react together.[18] The results show a much closer agreement between data and model in those runs done with $CuSO_4$ at pH 1.7, as seen in Figure 6. Furthermore, the model predicts that Cu(II) will increase the final Br_3^- yield by shutting off reaction 11(Br), while in the experiments, the opposite is observed. This suggests that there is an additional mechanism for oxidizing Br^- that involves HO_2, as unlikely as it may sound. Given the particularly low $HOONO_2$ concentrations used in spectrobromometry (cf. Table 2), a greater proportion of it would be expected to be dissociated into HO_2 and NO_2, thus enhancing both the relative importance of the Br^-/HO_2 chemistry and the system's likelihood of being disrupted by trace transition metals. We have determined that discrepancies could not be linked to uncertainties in either pH or H_2O_2 concentration. Similar experiments at pH 2.4 show greater differences between data and model, with or without additional copper (II).

Our experimental setup did not allow us to explore further the role of HO_2 in Br^- oxidation, but it clearly appears now that the model we present here is not quite complete and that radicals may also be involved in the oxidation process when the bromide concentration is high enough. Results show that $k_5(Br) = 0.54 \pm 0.08\ M^{-1}\ s^{-1}$ under catalytic conditions. We deem this number more reliable than the $0.60 \pm 0.18\ M^{-1}\ s^{-1}$ of semicatalytic experiments because it relies on simple linear regression, not on the complicated curve-fitting of eq II.

Chloride System. The challenge with the spectroiodometric study of this system was that Cl(0) oxidizes I^- all but instantly,[19] making it essentially indistinguishable from $HOONO_2$ itself. The spectroiodometric signal under such conditions is the sum of $HOONO_2$ and Cl(0) in the dilute reaction mixture, unless chlorine was reduced quickly enough by either reaction 11(Cl) or reaction 19.[20]

$$2H_2O_2 + Cl_2\ 6\ O_2 + 2Cl^- + 2H^+ \qquad (19)$$

H_2O_2 could theoretically have reduced Cl_2 to a significant extent in these experiments, but stoichiometric ratios, *S*, obtained by classical spectroiodometry suggest that if this reaction did occur, it was of limited extent, as *S* averaged to 0.26 ± 0.12 over 12 sets of experiments. It should nevertheless be noted that this is still larger than what was encountered with peroxynitric acid's thermal decay (0.03 ± 0.05). The radical-reduction model clearly showed that HO_2 could be an important reductant in this system, like it was in the iodide and bromide ones. It also indicated that Cl(0) should remain at trace levels throughout the experiments, making $HOONO_2$ the sole significant contributor to the spectroiodometric signal. Given such a mechanism, the oxidation of any single Cl^- ion should lead to the destruction of two $HOONO_2$ molecules. The chloride system was also expected to behave similarly to the bromide one in that the chloride would be regenerated by reaction 16(Cl), not reaction 15(Cl).

Preliminary experiments had hinted at a rate constant $k_5(Cl)$ of the order of $10^{-3}\ M^{-1}\ s^{-1}$. As such, the effect would be comparable to thermal decay only with $[Cl^-] \geq 10^{-1}$ M. Because fairly concentrated chloride solutions were to be used, constant ionic-strength was maintained by preparing dilute reaction mixtures with solutions of appropriate NaCl and $NaNO_3$ concentrations. The default ionic strength was 3.0 M. Initial $HOONO_2$ concentrations averaged to 1.8 ± 0.2 mM in classical-spectroiodometry experiments and to 0.46 ± 0.02 mM in flow-spectroiodometry ones, whereas the NaCl concentration was usually varied between 0.25 and 3.0 M.

There was no clear pH dependence in flow-spectroiodometry experiments between pH 1.16 and 3.27. The average rate constant was $k_5(Cl) = (1.4 \pm 0.4) \times 10^{-3}\ M^{-1}\ s^{-1}$ at $\mu = 3.0$ M. It was found by classical spectroiodometry that the reaction was enhanced by increasing ionic strength (see Figure 7), μ, according to the equation $k_5(Cl) = (6.0 \pm 2.3) \times 10^{-4}\ M^{-1}\ s^{-1} + (1.7 \pm 1.0) \times 10^{-4}\ M^{-2}\ s^{-1}\ \mu$. Finally, the temperature dependence is shown in Figure 8. The Arrhenius equation for this reaction was $k_5(Cl) = (4.8 \pm 2.9) \times 10^7\ M^{-1}\ s^{-1} \exp(-60 \pm 19\ kJ\ mol^{-1}/(RT))$.

Seawater−NaCl/KBr System. Some experiments were carried out with a mixture of NaCl and KBr in a 700:1 molar ratio, similar to the ratio found in sea salt.[21] The objective was to determine whether there could be synergetic effects in these halides' reactions with $HOONO_2$. They were otherwise identical to the chloride system experiments.

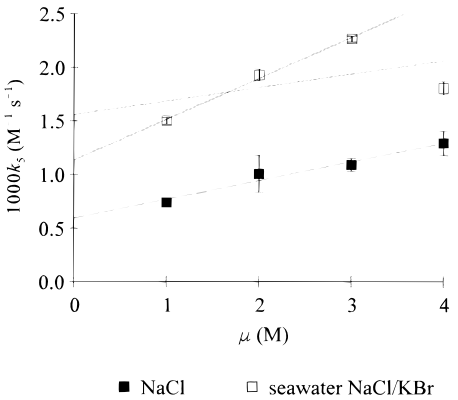

Figure 7. Influence of ionic strength on reactions 5(Cl) and 5(sw-Cl) at pH 1.3 ± 0.3 and 25.0 °C for 2.4 ± 0.6 mM (■) and 0.6 ± 0.1 mM $HOONO_2$ (□), respectively. Two linear regression fits are presented for the seawater data: both with and without taking into account k_5-(sw-Cl) at $\mu = 4$ M. Error bars represent one sample standard deviation.

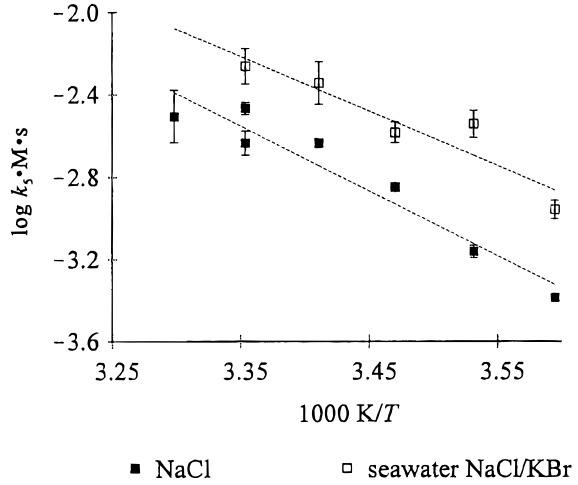

Figure 8. Arrhenius plots for reactions 5(Cl) and 5(sw-Cl) at $\mu = 3.0$ M and pH 3.25 ± 0.05 with 0.5 mM $HOONO_2$. Error bars represent one sample standard deviation.

Theoretically, $HOONO_2$ decay kinetics should obey eq III, where $k_{thermal}$ is the observed first-order rate constant for thermal decay. Since $[Cl^-]$:$[Br^-]$ was kept constant, the observed second-order rate constants k_5(sw-Cl) will be reported as a function of $[Cl^-]$, eq IV.

$$\frac{d[HOONO_2]}{dt} = -(k_{thermal} + 2k_5(Cl)[Cl^-] + 2k_5(Br)[Br^-])[HOONO_2] \quad \text{(III)}$$

$$k_5(sw{-}Cl) = k_5(Cl) + \frac{k_5(Br)}{700} \quad \text{(IV)}$$

The pH did not seem to have a significant influence in flow spectroiodometry experiments, with k_5(sw-Cl) averaging to (2.4 ± 0.5) × 10^{-3} M^{-1} s^{-1} Equation IV can be rearranged to extract k_5(Br) from k_5(Cl) and k_5(sw-Cl), leading to k_5(Br) = 0.7 ± 0.5 M^{-1} s^{-1}, in agreement with previous experiments.

Figure 7 illustrates the ionic-strength dependence of this system as found by flow spectroiodometry. The great difference with the chloride-only system is the trend reversal around 3 M. The main question is whether to include the point at $\mu = 4$ M from the seawater experiments. If it is included, subtracting the $k_5(Cl) = (1.4 \times 0.4) \times 10^{-3}$ M^{-1} s^{-1} value found previously from the intercept ($\mu = 0$ M) and using eq IV leads to k_5(Br) = 0.7 ± 1.0 M^{-1} s^{-1}, and without it, to k_5(Br) = 0.4 ± 0.4 M^{-1} s^{-1}. Despite the large uncertainties in both cases, the results are still comparable to what has been found with catalytic and semicatalytic experiments in bromide systems. Thus, $HOONO_2$ decay seems to obey eq III without evidence of any synergism.

TABLE 3: Comparison of $HOONO_2$/HSO_5^- + X^- Kinetics[a]

	$HOONO_2$	HSO_5^-
k_5(Cl)	1.4×10^{-3} M^{-1} s^{-1}	1.80×10^{-3} M^{-1} s^{-1}
k_5(Br)	0.6 M^{-1} s^{-1}	1.04 M^{-1} s^{-1}
k_5(I)	890 M^{-1} s^{-1}[a]	"instantaneous"
$dk_5(Cl)/d\mu$	1.7×10^{-4} M^{-2} s^{-1}	1.3×10^{-3} M^{-2} s^{-1}
ΔH_{a5}(Cl)	59 kJ mol^{-1}	60 kJ mol^{-1}

[a] $HOONO_2$ data: this work. HSO_5^- data: ref 22.

While finding the Arrhenius parameters for such a system is physically meaningless, determining them empirically can prove useful when evaluating halide oxidation in actual sea-salt aerosol particles. The data are presented in Figure 8 and the observed Arrhenius equation is k_5(sw-Cl) = (4.5 ± 3.7) × 10^6 M^{-1} s^{-1} exp(−51 ± 36 kJ mol^{-1}/(RT)).

Overall, the behavior of the seawater−NaCl/KBr system is consistent with what would be expected from the simple sum of the $HOONO_2$ chemistries with chloride and bromide. Furthermore, the data support the results of the catalytic and semicatalytic experiments in the bromide system, at least for conditions representative of the sea-salt aerosol.

Comparison with HSO_5^-. A peroxide analogue to $HOONO_2$ is peroxymonosulfuric acid (HSO_5^-), or Caro's acid. This compound's oxidation of halides follows the same pattern seen with peroxynitric acid, both qualitatively and quantitatively.[22] Table 3 shows how close the kinetic behavior of the peroxides are for both the rate constants and activation enthalpies for reaction 5 and its HSO_5^- equivalent. The only great difference is the influence of ionic strength for reaction 5(Cl). It can be readily explained by the fact that the negatively charged HSO_5^- will be much more sensitive to it than the neutral $HOONO_2$ molecule.

In this work, reaction 5 has been seen as an elementary, rate-determining step, involving a nucleophilic attack by the X^- ion on the hydrogen-bearing oxygen atom in $HOONO_2$, making HOX and NO_3^- as primary products. This was also one of the two possible mechanisms retained by Goldstein and Czapski for reaction 5(I),[15] as well as the one discussed by Fortnum et al. for a wide range of analogous peroxide−halide oxidations.[22] The latter also point out that "{I^-} is about a million times more reactive in attack on oxygen than is {Cl^-}". If k_5(I) and k_5(Cl) are compared, it can be seen that they differ by a factor 6 × 10^5. All this would place peroxynitric acid on par with Caro's acid in their peroxide reactivity series, i.e., H_2O_2 < $H_2PO_5^-$ < $CH_3C(O)OOH$ < $HOONO_2$, HSO_5^- < H_3PO_5.

Atmospheric Implications. In the marine boundary layer, halide oxidation by $HOONO_2$ in sea-salt particles should occur in two steps: mass transport of gas-phase $HOONO_2$ to the particles and aqueous-phase oxidation of dissolved halides. Mass transport depends on several factors such as particle number concentration and the gas-phase diffusion coefficient. While most of these had to be estimated, their values are expected to lie within well-known ranges. This allowed us to determine that the rate-limiting step in the whole oxidation process would be the aqueous-phase oxidation of halides, not the mass transport. The characteristic times[23] for these two processes are of the order of 10^7 and 10^3 s, respectively. We assumed that the particles' pH would remain around 2.5−3.5, as calculated by Keene and Savoie;[24] above that, the fast NO_4^- decay would

TABLE 4: Mixing Ratios Used in Evaluating Atmospheric Impact and Gas-Phase Halogen Atom Production Rates (atoms cm^{-3} h^{-1})[a]

	polluted	clean	
T (K)	293	293	273
NO_2(g) (ppt)	2000	10	10
$HOONO_2$(g) (ppt)	30	0.15	3
O_3(g) (ppb)	100	20	20
HCl(g) (ppt)	200	200	500
halogen atoms production rates			
(23) $O_3 + Br^- + H^+ \rightarrow O_2 + HOBr$	2×10^5	4×10^4	3×10^4
(5) $HOONO_2 + X^- \rightarrow NO_3^- + HOX$	1×10^6	7×10^3	2×10^5
(24) $2NO_2 + Cl^- \rightarrow NO_3^- + NOCl$[a]		($\leq 8 \times 10^9$)	
(25) $OH + HCl \rightarrow H_2O + Cl$	1×10^7	1×10^7	3×10^7

[a] For all conditions: 20 ppt HO_2(g), [Cl$^-$] = 3 M, [Cl$^-$]/[Br$^-$] = 700, [OH(g)] = 10^6 cm^{-3}. [b] Taken directly from ref 30, where a case with 50 ppb NO_2(g) at 20 °C was considered.

start to compete efficiently with halide oxidation and, at pH near 7−8, it could become fast enough to make mass transport rate-limiting. Given the molar ratio of Cl$^-$ and Br$^-$ in seawater, both anions should be oxidized at roughly equal rates by $HOONO_2$.

It is important to note here that as long as there are significant levels of bromide in the aerosol, any chloride oxidized to HOCl will in turn produce BrCl/$BrCl_2^-$ through reactions −6 and 20−22[17,25] before it has time to evaporate to the gas phase. The appropriate rate and equilibrium constants are listed in Table 1.

$$HOCl(aq) + Br^- \rightarrow BrCl(aq) + OH^- \quad (20)$$

$$Cl_2(aq) + Br^- \rightarrow BrCl_2^- \quad (21)$$

$$BrCl(aq) + Cl^- \rightleftharpoons BrCl_2^- \quad (22)$$

The question now remains to determine whether $HOONO_2$ can compete efficiently with other atmospheric oxidants for the production of gas-phase halogens. For our calculations, we chose sea-salt aerosol conditions of 1.0 particle per cubic centimeter with a size distribution characterized by a median radius of 1.6 μm and a logarithmic standard deviation of 0.5.[26] Sea-salt particles tend to lose water and become quite concentrated;[27] a value of 3 M was chosen for both μ and [Cl$^-$], corresponding to a relative humidity of about 90%. Table 4 lists typical mixing ratios of important species under a variety of conditions. Clean conditions would be those expected in remote tropical areas, like the central Pacific Ocean, while polluted ones would be more characteristic of the U.S. East Coast. Colder (273 K) clean conditions were also considered, as they would enhance peroxynitric acid's solubility and thus its potential impact.

We chose to compare four different daytime processes for the release of gas-phase halogen atoms (Cl or Br), namely (1) direct aqueous-phase bromide oxidation by ozone, (2) aqueous-phase halide oxidation by $HOONO_2$, (3) aqueous-phase chloride oxidation by NO_2, and (4) homogeneous gas-phase hydrogen abstraction from HCl by OH.

O_3 may be the single most important nonradical, daytime sea-salt halide oxidant. While it is not particularly efficient with Cl$^-$, it can oxidize Br$^-$ at an appreciable rate, reaction 23. We

$$O_3 + Br^- + H^+ \rightarrow O_2 + HOBr \quad (23)$$

tried to estimate under what conditions would peroxynitric acid oxidize halides more efficiently than does ozone. Equation V shows the condition for the two to be equal. k_5(sw-Cl) is again the observed second-order rate constant in seawater as in eq IV, H_{HOONO_2} and H_{O_3} are the Henry's law constants, K_{1g} is the equilibrium constant for reaction 1 in the gas-phase,[28] n_o is a unit-conversion factor equal to 7.34 × 10^{21} molecules cm^{-3} atm^{-1} K/T, and p_{O_3} is the gas-phase ozone partial pressure.

TABLE 5: Values for the Variables of Eq V

variable	value	ref
K_{1g}	(7.3×10^{27} molecule cm^{-3}) exp(−11700/T)	28
k_5(sw-Cl)	(4.5×10^6 M^{-1} s^{-1}) exp(−6100/T)	this work
k_{23}	(6.3×10^8 M^{-1} s^{-1}) exp(−4450/T)	18
H_{HOONO2}	(1.3×10^{-6} M atm^{-1}) exp(6870/T)	10
H_{O3}	(2.2×10^{-6} M atm^{-1}) exp(2560/T)	25
n_o	$N_A/R = 7.34 \times 10^{21}$ molecules cm^{-3} atm^{-1} K	

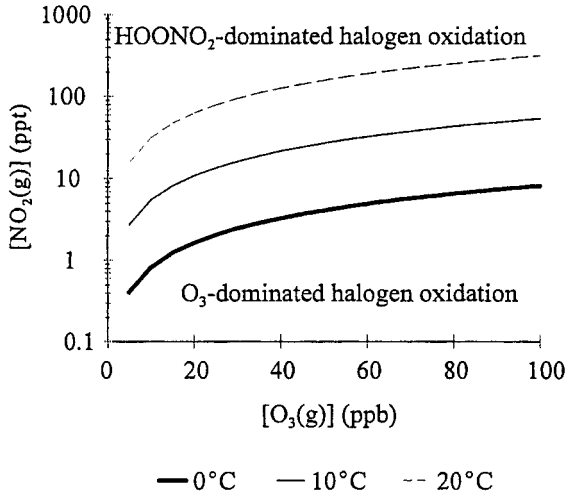

Figure 9. Oxidation chemistry of halides in sea-salt aerosol with 20 ppt HO_2(g). The lines represent the conditions under which $HOONO_2$ and O_3 will oxidize halides at equal rates for the given temperature. Acid dissociation of $HOONO_2$ has been ignored.

$$k_5(\text{sw-Cl})(H_{OONO_2}(K_{1g}^{-1}[HO_2(g)][NO_2(g)]/n_o))[Cl^-] = k_{22}(H_{O_3}p_{O_3})[Br^-] \quad (V)$$

With $p_{O_3}n_o = [O_3(g)]$, one can rearrange eq V to isolate [NO_2(g)]/[O_3(g)]; taking into account the temperature dependencies of the rate and equilibrium constants (cf. Table 5) eventually leads to eq VI. This equation was then used to give Figure 9

$$\frac{[NO_2(g)]}{[O_3(g)]} \approx (1.7 \times 10^{30}\ \text{cm}^3\ \text{molecule}^{-1})e^{-1.44\times10^4\text{K}/T}\left(\frac{[Br^-]}{[HO_2(g)][Cl^-]}\right) \quad (VI)$$

which shows the conditions under which either oxidant dominates the chemistry. Above the lines, i.e., in cold, NO_2-rich atmospheres, $HOONO_2$ oxidizes more halides than ozone; below the lines, O_3 dominates. In remote tropical oceans, ozone would be expected to be the dominant oxidant. As the aerosol's bromide becomes depleted, ozone chemistry will gradually lose its importance, until it is replaced by peroxynitric acid's direct oxidation of chloride. We did not consider the complex mechanism proposed by Oum et al., where O_3 acts essentially as a source of aqueous-phase H_2O_2.[29]

Assuming steady-state, $HOONO_2$ could conceivably release 10^6 halogen atoms cm^{-3} h^{-1} in polluted conditions at 293 K, with colder temperatures favoring a greater production. By comparison, bromide oxidation by 100 ppb of ozone would

produce 2×10^5 halogen atoms cm^{-3} h^{-1} from fresh sea-salt aerosol. Further comparison are included in Table 4.

NO_2 might also be a significant daytime producer of gas-phase Cl radicals. Karlsson and Ljungström have studied reaction 24 and claim that up to 10^7 Cl atoms cm^{-3} h^{-1} might

$$2NO_2 + Cl^- \rightarrow NO_3^- + NOCl(aq) \qquad (24)$$

have been released through it, provided NOCl does not hydrolyze before evaporating.[30] Nevertheless, we must express some reserves concerning their work. Assuming a rate-limiting step that is first order in both reactants, the implicit conclusion of their work is that $k_{24} \approx 140$ M^{-1} s^{-1} at 20 °C. With 10^{-4} to 10^{-3} M $HOONO_2$ levels typical of the systems we studied, equilibrium 1 and reactions 2 and 3 imply that some 10^{-7} M $NO_2(aq)$ was present at steady state. Given our experimental conditions in the chloride system, reaction 24 would have been enough to make $HOONO_2$ decay 1 order of magnitude faster than was observed.

So far, the only well-established daytime source of chlorine atoms in the marine boundary layer is homogeneous-gas-phase reaction 25. Given typical HCl mixing ratios of 100−300 ppt

$$OH(g) + HCl(g) \rightarrow H_2O(g) + Cl(g) \qquad (25)$$

in remote marine areas,[31] 10^6 OH molecules cm^{-3}, and $k_{25} = 8.0 \times 10^{-13}$ cm^3 $molecule^{-1}$,[32] it could produce $(0.7-2) \times 10^7$ Cl atoms cm^{-3} h^{-1}. These numbers are expected to be even higher in coastal areas, especially those suffering from anthropogenic pollution; for example, Keene et al. measured up to 1200 ppt HCl off the U.S. East Coast.[5] This gas-phase Cl production is much larger than what can reasonably be expected from direct halide oxidation by either ozone or peroxynitric acid, making the latter at best a marginal player in marine boundary layer halogen chemistry even in polluted conditions, unless temperatures are particularly cold.

Finally, nighttime reaction 26 was also considered, as it can produce large quantities of $ClNO_2$ ready to be photolyzed at sunrise. With a realistic level of 0.5 ppb N_2O_5 for polluted

$$N_2O_5 + Cl^- \rightarrow NO_3^- + ClNO_2(g) \qquad (26)$$

coastal conditions[33] and a reaction probability γ of 0.03,[34] a flux of 4×10^9 molecules cm^{-3} h^{-1} could be expected, much larger than any of the daytime reactions considered in the present work. As the air gets farther offshore and cleaner, NO_x levels will sharply fall and so will N_2O_5 and this production pathway.

As it stands, $HOONO_2$ cannot directly account for the oxidized halogens present in the marine boundary layer. If it is linked in any way to them, it must be by initiating some autocatalytic cycles, as suggested Vogt et al.[8] and Sander and Crutzen.[25] Only further modeling studies may elucidate its part in the whole process.

Conclusion

So far, it has been possible to find reliable values for $k_5(X)$ with all three halide systems studied in this work. The results show that $HOONO_2$ is kinetically very close to HSO_5^- as a halide oxidant. We have demonstrated that $HOONO_2$ also has a significant reductive capacity toward halogen molecules, not directly but rather through the HO_2 in equilibrium with it.

There are areas of these systems' chemistry that still elude us. First, the observed iodine mass balance in the near-stoichiometric range is incomplete and suggests the formation of a reservoir that could conceivably survive a long time under these conditions. Second, systems with high bromide concentrations ($\geq 10^{-2}$ M) show irreproducible behavior as well as an accelerated oxidation that appears to be related to HO_2. Finally, while there is little doubt that HO_2 is the dominant X_2 reductant in all three systems, a significant if secondary role for H_2O_2 has not been totally ruled out yet, for observed stoichiometric ratios are definitely greater than those found in peroxynitric acid's thermal decay.

Basic calculations show that $HOONO_2$ cannot be a significant player in the daytime oxidation of sea-salt halides without the combination of a polluted, NO_2-rich atmosphere and cold temperatures. Even then, homogeneous gas-phase production of chlorine atoms from reaction 25 is expected to be much more important. Modeling studies would be needed to determine whether it can reasonably be expected to play a role in initiating halogen-releasing autocatalytic cycles.

Acknowledgment. We thank the Natural Sciences and Engineering Research Council of Canada for funding.

Supporting Information Available: Lists of values plotted in Figures 3, 4, 6, 7, and 8. Lists of measured values of k_5(Br), k_5(Cl), and k_5(sw-Cl) values as a function of pH. This material is available free of charge via the Internet at http://pubs.acs.org.

References and Notes

(1) Eriksson, E. *Tellus* **1960** *12*, 74.
(2) Pszenny, A. A. P.; Keene, W. C.; Jacob, D. J.; Fan, S.; Maben, J. R.; Zetwo, M. P.; Springer-Young, M.; Galloway, J. N. *Geophys. Res. Lett.* **1993**, *20*, 699.
(3) Spicer, C. W.; Chapman, E. G.; Finlayson-Pitts, B. J.; Plastridge, R. A.; Hubbe, M. M.; Fast, J. D.; Berkowitz, C. M. *Nature* **1998**, *394*, 353.
(4) Bottenheim, J. W.; Barrie, L. A.; Atlas, E.; Heidt, L. E.; Niki, H.; Rasmussen, R. A.; Shepson, P. B. *J. Geophys. Res.* **1990**, *95*, 18, 555.
(5) Keene, W. C.; Pszenny, A. A. P.; Jacob, D. J.; Duce, R. A.; Galloway, J. N.; Schultz-Tokos, J. J.; Sievering, H.; Boatman, J. F. *Global Biogeochem. Cycles* **1990**, *4*, 407.
(6) Graedel, T. E.; Keene, W. C. *Global Biogeochem. Cycles* **1995**, *9*, 47.
(7) Oum, K. W.; Lakin, M. J.; DeHaan, D. O.; Brauers, T.; Finlayson-Pitts, B. J. *Science* **1998**, *279*, 74.
(8) Vogt, R.; Crutzen, P. J.; Sander, R. *Nature* **1996**, *383*, 327.
(9) Kurylo, M. J.; Ouellette, P. A. *J. Phys. Chem.* **1986**, *90*, 441.
(10) Régimbal, J.-M.; Mozurkewich, M. *J. Phys. Chem. A* **1997**, *101*, 88822.
(11) Løgager, T.; Sehested, K. *J. Phys. Chem.* **1993**, *97*, 10, 047.
(12) Appelman, E. H.; Gosztola, D. J. *Inorg. Chem.* **1995**, *34*, 787.
(13) Goldstein, S.; Czapski, G.; Lind, J.; Merenyi, G. *Inorg. Chem.* **1998**, *37*, 3943.
(14) Awtrey, A. D.; Connick, R. E. *J. Am. Chem. Soc.* **1951**, *73*, 1842.
(15) Goldstein, S.; Czapski, G. *Inorg. Chem.* **1997**, *36*, 4156.
(16) Jouanne, J. v.; Keller-Rudek, J.; Kuhn, P.; List, H.; Merlet, P.; Ruprecht, S.; Vanecek, H.; Wagner, J. *Gmelin Handbook of Inorganic Chemistry*, 8th ed.; Br, Supplement Volume A, Element; Koschel, D., Ed.; Springer−Verlag: Berlin, 1985; pp 455−456.
(17) Wang, T. X.; Delley, M. D.; Cooper, J. N.; Beckwith, R. C.; Margerum, D. W. *Inorg. Chem.* **1994**, *33*, 5872.
(18) Ross, A. B.; Bielski, B. J. J.; Baxton, G. V.; Cabeli, D. E.; Greenstock, C. L.; Helman, W. P.; Huie, R. E.; Grodkowski, J.; Neta, P. *NIST Standard Reference Database 40, NDRL/NIST Solution Kinetics Database, Version 2.0*; NIST Standard Reference Data: Gaithersburg, MD, 1994.
(19) Lister, M. W.; Rosenblum, P. *Can. J. Chem.* **1963**, *41*, 3013.
(20) Connick, R. E. *J. Am. Chem. Soc.* **1947**, *69*, 1509.
(21) Seinfeld, J. H.; Pandis, S. N. *Atmospheric Chemistry and Physics, From Air Pollution to Climate Change*; John Wiley & Sons: New York, 1998; 1326 pp.
(22) Fortnum, D. H.; Battaglia, C. J.; Cohen, S. R.; Edwards, J. O. *J. Am. Chem. Soc.* **1960**, *82*, 778.
(23) Schwartz, S. E.; Freiberg, J. E. *Atmos. Environ.* **1981**, *15*, 1129.
(24) Keene, W. C.; Savoie, D. L. *Geophys. Res. Lett.* **1998**, *25*, 2181.
(25) Sander, R.; Crutzen, P. J. *J. Geophys. Res.* **1996**, *101*, 9121.
(26) Kim, Y.; Sievering, H.; Boatman, J. *Global Biogeochem. Cycles* **1990**, *4*, 165.
(27) Ravishankara, A. R. *Science* **1997**, *276*, 1058.

(28) Zabel, F. *Z. Phys. Chem.* **1995**, *188*, 119.
(29) Oum, K. W.; Lakin, M. J.; DeHaan, D. O.; Brauers, T.; Finlayson-Pitts, B. J. *Science* **1998**, *279*, 74.
(30) Karlsson, R.; Ljunström, E. *Atmos. Environ.* **1995**, *26*, 39.
(31) Graedel, T. E.; Keene, W. C. *Global Biogeochem. Cycles* **1995**, *9*, 47.
(32) DeMore, W. B.; Sander, S. P.; Golden, D. M.; Hampson, R. F.; Kurylo, M. J.; Howard, C. J.; Ravishankara, A. R.; Kolb, C. E.; Molina, M. J. *Chemical Kinetics and Photochemical Data for Use in Stratospheric Modeling*; JPL publ. 92−20; Jet Propulsion Laboratory: Pasadena, CA, 1992.
(33) Heintz, F.; Platt, U.; Flentje, H.; Dubois, R. *J. Geophys. Res.* **1996**, *101*, 22891.
(34) Behnke, W.; George, C.; Scheer, V. Zetzsch, C. *J. Geophys. Res.* **1997**, *102*, 3795.
(35) Halfpenny, E.; Robinson, P. L. *J. Chem. Soc. A* **1952**, 928.
(36) Bielski, B. H. J.; Cabelli, D. E.; Arudi, R. L.; Ross, A. B. *J. Phys. Chem. Ref. Data* **1985**, *14*, 1041.
(37) Eigen, M.; Kustin, K. *J. Am. Chem. Soc.* **1962**, *84*, 1355.
(38) Ruasse, M.-F.; Aubard, J.; Galland, B.; Adenier, A. *J. Phys. Chem.* **1986**, *90*, 4382.
(39) Liebhafsky, H. A.; Mohammad, A. *J. Am. Chem. Soc.* **1933**, *55*, 3977.
(40) Mohammad, A.; Liebhafsky, H. A. *J. Am. Chem. Soc.* **1934**, *56*, 1680.
(41) . Liebhafsky, H. A. *J. Am. Chem. Soc.* **1932**, *54*, 1792.
(42) Young, H. A. *J. Am. Chem. Soc.* **1950**, *72*, 3310.